

Final Report: MESSENGER Spacecraft Level DC Magnetic Field Test Results

B. J. Anderson 7/19/2004

Summary

The fixed magnetic field of the MESSENGER spacecraft was characterized using measurements taken on 28 November 2003. The tests consisted in measuring the magnetic field near the spacecraft with three field-test magnetometers while the unpowered spacecraft was suspended from an overhead crane, displaced $\sim 4^\circ$ from vertical, released and allowed to swing in free pendulum motion for five or more oscillations. A total of sixteen such pendulum oscillation sets of measurements were taken with the spacecraft and field-test magnetometers in different orientations and positions both to ensure complete coverage of the spacecraft near-field and to distinguish the spacecraft permanent moment from any moment induced by the presence of permeable materials in Earth's field. The results gave no evidence for an induced moment and agree with a quantitative model for the spacecraft field based on the propulsion system latch valves, thrusters and custom cancellation magnets installed to compensate for the magnetic field at the position of the deployed science magnetometer sensor. The observations and model agree to within 20%, comparable to the uncertainties and possible systematic biases in the tests and analysis. Calculating the model field without the compensation magnets gives strong disagreement with the observations. The agreement of the complete model and the test measurements demonstrates: (1) that there are no major sources of spacecraft magnetic field other than those identified during integration and incorporated into the spacecraft field model; (2) that the compensation magnets were installed properly; and (3) that the spacecraft magnetic field model provides a useful quantitative estimate of the spacecraft field. The magnetic field magnitude at the location of the stowed sensor is estimated to be 220 ± 44 nT indicating that the flight instrument should be operable in its sensitive range (± 1024 nT) during cruise prior to and during boom deployment.

1. Introduction

To ensure that the MESSENGER magnetic field science objectives will be met, a magnetics program was followed both for fixed and variable field sources. This report describes the final pre-launch measurements of the spacecraft fixed magnetic field performed as part of the magnetics cleanliness program. To mitigate the effects of fixed field sources, all magnetic components on the spacecraft were assessed, first by determining if they possessed a significant moment, and if necessary measuring their moments accurately. It turned out that the propulsion latching valves were by far the dominant fixed magnetic field source and their moments were measured to 1% accuracy at the JHU/APL magnetics facility. Figure 1 shows the spacecraft viewing the +XSC side where the propulsion latching valves are plainly visible. The thrusters have moments less than $1/20^{\text{th}}$ of the valves and their moments were measured to 10% accuracy at Aerojet Corp. No other components tested possessed moments large enough to contribute more than 0.1 nT at the MESSENGER magnetometer sensor deployed location.

A quantitative model of the spacecraft magnetic field was created using the propulsion latch valve and thruster moments. Specific locations for two cancellation magnets were identified and the magnetic field model was used to design cancellation magnets that would yield minimum field at the deployed location of the magnetometer. Two magnets were custom built to the moments specified by the model and installed on the spacecraft. The spacecraft magnetic

field model, including the cancellation magnets, is important because it will be used to predict the magnetic field measured during boom deployment which is the only direct signature of boom deployment.

The science objectives do not require that the residual field be precisely determined prior to launch. Because post-launch calibrations can provide this information, it was only necessary to show that the spacecraft will have a small fixed residual magnetic field at the deployed sensor location. Thus, it was not necessary to do a detailed spacecraft magnetics characterization and total moment cancellation. Rather, final measurements of the spacecraft magnetic field were conducted to ensure that the magnetics program had been successful. The test objectives were: (1) to establish that all major sources of fixed magnetic fields had been identified, that is, to ensure that nothing had been overlooked; (2) to verify that the cancellation magnets were installed properly, for example, that they were not put on backwards; (3) to test the spacecraft magnetic field model. The propulsion system, battery, avionics systems and payload were all integrated prior to the tests described here. The solar arrays, sun-shade fabric, thermal

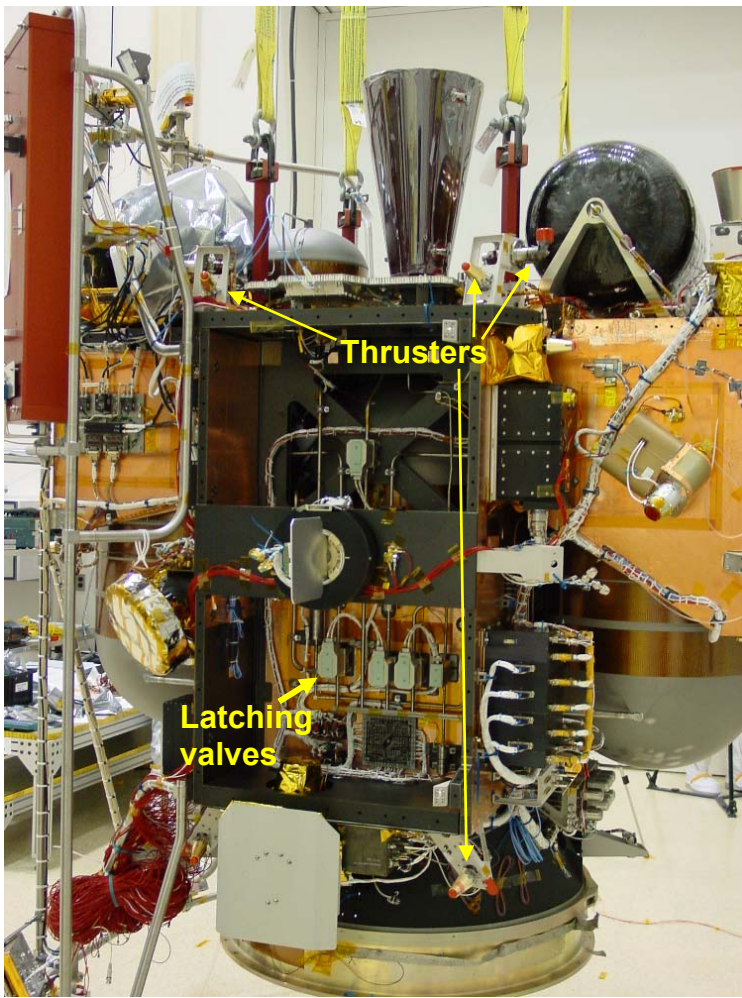


Figure 1. View of the spacecraft +X side showing several of the propulsion latching valves and thrusters.



Figure 2. Spacecraft lift fixture and crane hook.

blankets and stainless steel Velcro used to attach the sun-shade fabric were the only elements not installed for this test. The solar arrays and Velcro were all demagnetized prior to their subsequent integration with the spacecraft. The sunshade fabric and thermal blanket materials were established to be non-magnetic as part of the thermal design early in development.

2. Test Description

2.1 Overview

The test consisted of suspending the spacecraft from the overhead crane in the high-bay area of the integration and assembly building and measuring the magnetic field with three field-test magnetometers while the spacecraft swung gently in pendulum fashion. The magnetic field variations are due to the spacecraft. The complete test used a series of measurements at different locations, for different directions of pendulum motion and for two orientations of the spacecraft rotated about the vertical. The entire set of measurements allowed us to establish how much of the magnetic field is due to permanent magnets (>90%), how much is from permeable materials (<10%), and to quantitatively test the specific predictions of the spacecraft magnetic field model to meet all of the test objectives.



Figure 3. Spacecraft, lift fixture and crane prior to separation from integration fixture.



Figure 4. Spacecraft suspended from lift fixture at the North end of high bay. Test magnetometer and tripod can be seen to the right (East) of the spacecraft.

Figure 2 shows the crane, crane hook, lift fixtures and straps used for the test. All of the steel hardware, below and including the steel triangle (red) to which the four upper straps are attached, including shackles, eye-bolts and the square spreading fixture, were demagnetized prior to the test. No attempt was made to demagnetize the larger hardware, for example the crane hook. Figure 3 shows the spacecraft and lift fixture just prior to lifting the spacecraft off of the integration fixture. Figure 4 shows the spacecraft suspended from the crane after transiting to the opposite end of the high bay area. The large silver duct is an air conditioning line used to keep the battery cool. The tests were conducted without this duct in place and the total time allowed for the testing was limited to a maximum of three hours to prevent the battery from warming above allowed limits. The actual magnetics measurements took less than one hour to complete.

2.2. Measurement Setup

The magnetometer test equipment consisted of three identical magnetometers operated by laptop computers via AD/DAC cards, power converter electronics and controlled by LabView software which recorded, displayed and saved the data. Figure 5 shows the two laptops used during the test. One laptop controlled two magnetometers, MAG-A which was mounted on a



Figure 5. Dual laptops running the three field-test magnetometers. Mag A 1 (floor) and A 2 (tripod A) are run off the laptop to the right. MAG B (tripod B) was run off the laptop to the left.



Figure 6. Field-test magnetometer B mounted on a camera tripod. The magnetometer is the black rectangular box at the left upper end of the aluminum box channel. The orange wire windings provide a timing signal in the magnetic field data stream.

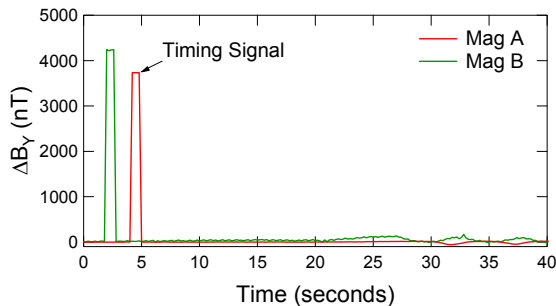


Figure 7. Timing signal generated in MAG-A and MAG-B data to synchronize the signals in analysis.



Figure 8. Measuring the height of the spacecraft adapter fitting above the floor. MAG-FLR can be seen underneath the spacecraft.

tripod five feet above the floor, and MAG-FLR which was placed on the floor approximately directly under the spacecraft. MAG-B was controlled by the second laptop. Figure 6 shows MAG-B on its tripod, also five feet above the floor. Rather than synchronizing the two laptops a timing signature was introduced in the data from MAG-A and MAG-B by placing windings connected in series over the active sensor portion of these instruments. A simple pushbutton switch and 9V battery were used to manually send a current through the windings generating a magnetic field pulse in the time series for MAG-A and MAG-B providing the necessary timing synchronization for the analysis. Figure 7 shows this timing pulse for one of the measurements.

The spacecraft position was recorded and controlled as follows. The height of the payload adapter fitting above the floor was measured (Figure 8) and was 19 inches. To specify and monitor the lateral position of the spacecraft a laser pointer was taped to the Sun-shield frame pointing vertically down to the floor. The pointer was taped in the ON position. This provided a reference rest point on the floor as shown in Figure 9. This laser spot was used to specify reproduce the spacecraft displacement prior to pendulum release by lining the laser spot up to a line marked 24 inches to the North or West of the equilibrium position. The laser spot also provided clear indication of whether the pendulum motion was linear or somewhat elliptical.

To organize the measurements a reference coordinate system was adopted in which X_S , Y_S and Z_S were positive South, East and up, respectively. The origin of this system was arbitrarily chosen to be on the floor at a point approximately centered between the East and West sides of the room and located by a seam in the flooring. MAG-FLR was placed close to the



Figure 9. Reference laser pointer and spot used to locate and reproduce equilibrium positions and displacement prior to release for pendulum swing motion.

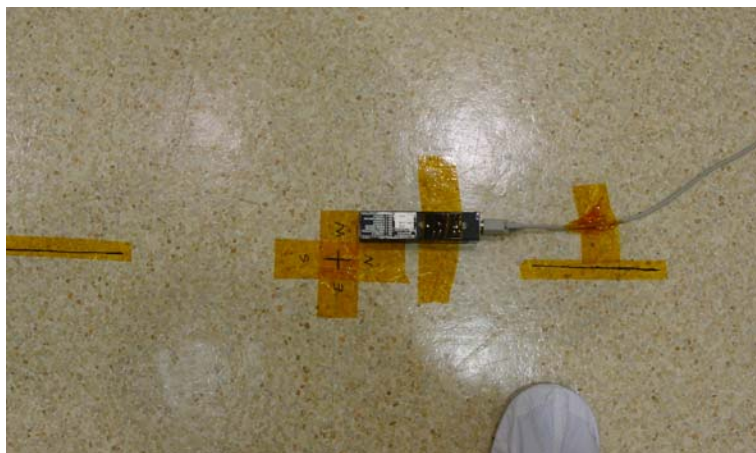


Figure 10. Floor magnetometer (MAG-FLR) in its location throughout the tests. N, S, E & W are indicated and the lines correspond to the test system X axis.

origin as shown in Figure 10. The positions of MAG-A/MAG-B were established using a plumb line on the test system X and Y axes and 60 inches above the floor. To reproduce the tipod positions the foot-points were marked on the floor. The coordinates of all field-test magnetometers in and the magnetometer axes directions relative to system coordinates in the reference system in each position were noted. These coordinates, relative to N-S/E-W and to spacecraft coordinates are indicated in Figure 11. Two spacecraft orientations were used, denoted 0° and 180° , which correspond to opposite orientations about the vertical. This was necessary to distinguish permanent sources from those due to permeable materials with little permanent moment

2.3. Spacecraft Pendulum Swing

A measurement sequence consisted of starting taking magnetometer data while the spacecraft was allowed to swing in pendulum motion. The specific steps were as follows. First the test magnetometer recordings were begun. The timing signal was then generated and then the bottom of the spacecraft was manually pulled by means of a nylon rope attached at the

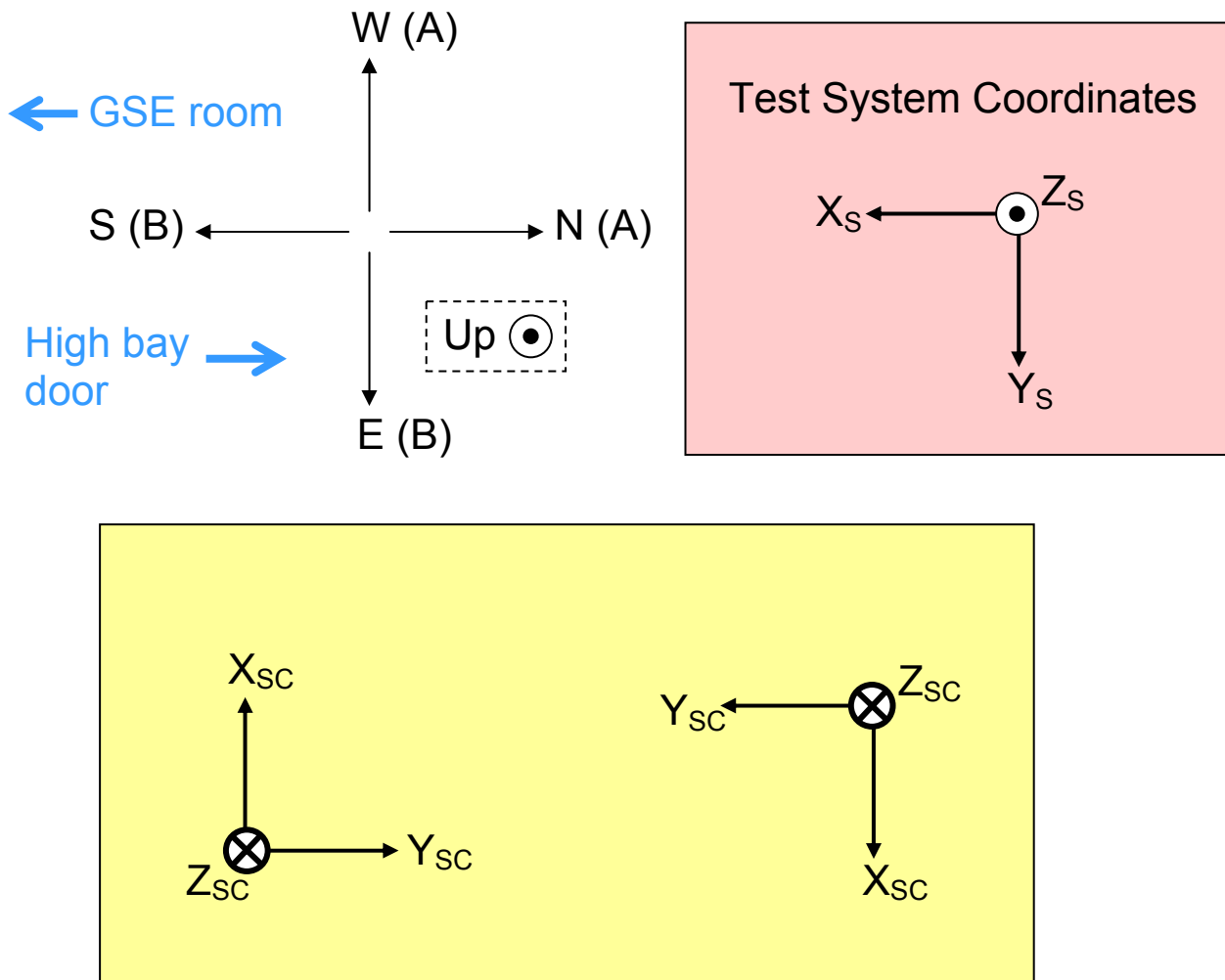


Figure 11. Coordinate systems relative to N/S E/W directions in the high bay area (upper left panel). MAG-A was positioned in two places, W and N of the origin and MAG-B was positioned diametrically opposite the origin from MAG-A, that is E and S (upper left panel). Test system coordinates remained fixed throughout the test (upper right panel). MAG-FLR remained on the floor near the test system origin throughout the tests. The two spacecraft orientations and the directions of spacecraft coordinates are indicated in the bottom panel.

bottom of the spacecraft adapter flange to displace the laser indicator spot 24 inches from its equilibrium position. Depending on the test step the displacement was either N-S or E-W. This displacement was maintained for some seconds to make sure the spacecraft, lift assembly and crane came to rest making a small angle, $\sim 4^\circ$ with respect to vertical. This is shown in the left hand panel of Figure 12. The technician then let go of the rope, releasing the spacecraft to swing in a gentle free pendulum motion shown in the right hand panel of Figure 12. Since the crane is approximately 30 feet high, the pendulum period was approximately 5 s, $\sim 2\pi\sqrt{(30 \text{ ft}/32 \text{ ft/s}^2)}$. Because the displacement was not strictly sideways but tangent to the spacecraft-crane line, the test did not result in significant lateral stresses on the spacecraft lift attach points. The pendulum motion was allowed to repeat for at least five complete periods and then damped by pulling gently on the bottom of the adapter flange. The process was repeated once so that each measurement step consisted of two such pendulum swing series.

2.4. Test Sequence

The complete test consisted of two series of measurement steps. In the first series, labeled 3_1, 3_2, 3_3 and 3_4, the spacecraft was in the 0° position as shown in Figure 13. The



Figure 12. Displacement of the spacecraft in the $+X_S, -Y_{SC}$, South direction (left) and about 1 second after release during the free pendulum motion (right).



Figure 13. Spacecraft in 0° orientation. MAG-A is to the left (North) and MAG-B is to the right (South).

second series labeled 5_1, 5_2, 5_3 and 5_4 the spacecraft was in the 180° position, shown in Figure 14. Table 1 lists the creation times of data files stored on the laptops, the filenames which include these step labels, the direction along which the tripod magnetometers were placed, and the direction in which the spacecraft pendulum motion occurred. In steps 3_1 and 3_2 the tripod magnetometers, A and B, were positioned along the N-S, X_S or Y_{SC} axis. In 3_1 the spacecraft pendulum direction was in the X_S direction, N-S, or toward and away from the tripod magnetometers. In 3_2 the spacecraft pendulum direction was in the Y_S direction, E-W, or lateral with respect to the X_S axis. For steps 3_3 and 3_4 the A and B magnetometers were positioned along the Y_S axis, (X_{SC} , E-W). In step 3_3 the spacecraft displacement was in the N-S direction, lateral relative to the tripod magnetometers. In 3_4 the spacecraft displacement was in the E-W direction, toward and away from the magnetometers.



Figure 14. Spacecraft in 180° orientation.

Table 1. Files, acquisition times, test magnetometer positions and SC swing directions.

EST	Filename	MAG	SC
09:24a	2003 1128 SC DC TEST TRPD1 B4 001.dat	E-W	N/A
10:20a	2003 1128 SC DC TEST TRPD1 B4 002.dat	E-W	N/A
10:24a	2003 1128 SC DC TEST 3 4 TRPDA 001.dat	E-W	E-W
10:32a	2003 1128 SC DC TEST 3 3 TRPDA 001.dat	E-W	N-S
10:39a	2003 1128 SC DC TEST 3 1 TRPDA 001.dat	N-S	N-S
10:44a	2003 1128 SC DC TEST 3 2 TRPDA 001.dat	N-S	E-W
10:59a	2003 1128 SC DC TEST 5 3 TRPDA 001.dat	N-S	N-S
11:03a	2003 1128 SC DC TEST 5 4 TRPDA 001.dat	N-S	E-W
11:09a	2003 1128 SC DC TEST 5 2 TRPDA 001.dat	E-W	E-W
11:13a	2003 1128 SC DC TEST 5 1 TRPDA 001.dat	E-W	N-S
09:25a	2003 1128 SC DC TEST B4 TRPDB 001.dat	E-W	N/A
10:20a	2003 1128 SC DC TEST B4 TRPDB 002.dat	E-W	N/A
10:24a	2003 1128 SC DC TEST 3 4 TRPDB 001.dat	E-W	E-W
10:32a	2003 1128 SC DC TEST 3 3 TRPDB 001.dat	E-W	N-S
10:39a	2003 1128 SC DC TEST 3 1 TRPDB 001.dat	N-S	N-S
10:44a	2003 1128 SC DC TEST 3 2 TRPDB 001.dat	N-S	E-W
10:59a	2003 1128 SC DC TEST 5 3 TRPDB 001.dat	N-S	N-S
11:03a	2003 1128 SC DC TEST 5 4 TRPDB 001.dat	N-S	E-W
11:09a	2003 1128 SC DC TEST 5 2 TRPDB 001.dat	E-W	E-W
11:14a	2003 1128 SC DC TEST 5 1 TRPDB 001.dat	E-W	N-S

Because the spacecraft was moved into position from the South, the actual sequence of the tests was different from that originally envisioned. It turned out that steps 3_4 and 3_3 were

actually the first steps done because the tripods didn't have to be moved out of the way to allow the spacecraft through. The tripods were then repositioned to their N-S locations and steps 3_1 and 3_2 were done. The spacecraft was then rotated to its 180° orientation and steps 5_3 and 5_4 conducted. Finally, the tripods were moved back to their E-W positions and steps 5_1 and 5_2 were done.

3. Data Analysis

Analysis of the test data required careful specification of coordinate systems, examination of the data time series to identify the most important measurements, specification of the magnetometer positions in spacecraft coordinates at the extrema of spacecraft displacements, and evaluation of the spacecraft model. The model was evaluated along the approximate trajectory in spacecraft coordinates and differences between values at points corresponding to extrema in the displacement evaluated for comparison with the observations.

3.1. Coordinate Systems

The first step in the analysis was specification of the coordinates of each magnetometer at each step of the test. Figure 15 shows MAG-FLR and the directions of the positive sign of each axis for the instrument. These coordinates relative to the body of the magnetometer are the same for all three field-test magnetometers. The coordinates of MAG-FLR relative to test system coordinates obviously were the same throughout the test. Since the other magnetometers were repositioned and oriented differently for different tests, the relation of their axes to test system coordinates varied. Also, since the spacecraft was rotated 180° for the second set of steps, the relation of magnetometer coordinates to spacecraft coordinates was different for the first and second series of tests. Tables 2 and 3 give the directions in spacecraft coordinates of each axis of MAG-FLR, MAG-A and MAG-B for each step of the test. The coordinates in spacecraft coordinates (for the spacecraft at rest) in cm for each magnetometer and each step are given in Tables 4 and 5.

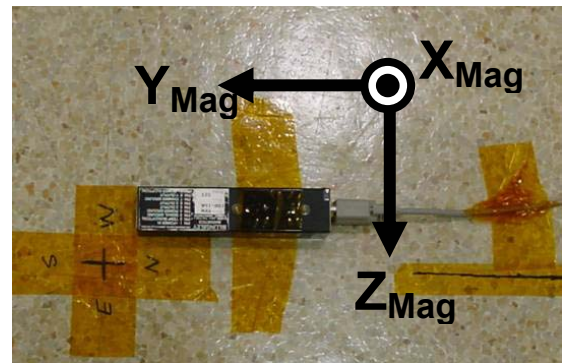


Figure 15. Close-up of MAG-FLR also showing the directions corresponding to the X, Y and Z axes of the magnetometer sensor.

Table 2. Conversions between spacecraft coordinates the test system and floor MAG coordinates.

SC orientation	Steps	X-S	Y-S	Z-S	X-Flr	Y-Flr	Z-Flr
0°	3_1,2,3,4	-Y-sc	-X-sc	-Z-sc	-Z-sc	-Y-sc	-X-sc
180°	5_1,2,3,4	+Y-sc	+X-sc	-Z-sc	-Z-sc	+Y-sc	+X-sc

Table 3. Conversions between spacecraft coordinates and MAG-A and MAG-B coordinates.

SC orientation	Mags	Steps	X-A	Y-A	Z-A	X-B	Y-B	Z-B
0°	N-S	3_1,2	-Z-sc	-Y-sc	-X-sc	-Z-sc	+Y-sc	+X-sc
0°	E-W	3_3,4	-Z-sc	-X-sc	+Y-sc	-Z-sc	+X-sc	-Y-sc
180°	E-W	5_1,2	-Z-sc	+X-sc	-Y-sc	-Z-sc	-X-sc	+Y-sc
180°	N-S	5_3,4	-Z-sc	+Y-sc	+X-sc	-Z-sc	-Y-sc	-X-sc

Table 4. Floor MAG Position in SC Coordinates (SC at rest).

SC orientation	Steps	Floor Mag (cm)		
		X-sc	Y-sc	Z-sc
0°	3_1,2,3,4	0	0	+64
180°	5_1,2,3,4	0	0	+64

Table 5. MAG-A and MAG-B Locations in SC Coordinates (SC at rest).

SC orientation	Mags	Steps	MAG-A (cm)			MAG-B (cm)		
			X-sc	Y-sc	Z-sc	X-sc	Y-sc	Z-sc
0°	N-S	3_1,2	0	+236	-91	0	-236	-90
0°	E-W	3_3,4	+236	0	-91	-236	0	-90
180°	E-W	5_1,2	-236	0	-91	+236	0	-90
180°	N-S	5_3,4	0	-236	-91	0	+236	-90

3.2. Spacecraft Displacement Direction

Table 1 gives the line along which the spacecraft was displaced for each step but not the initial direction. This direction is actually easily determined from the magnetic field data itself. For example, in step 3_1 the spacecraft is displaced along the line between MAG-A and MAG-B. Because the spacecraft magnetic field is due to a collection of dipoles which are designed to cancel at large distances the field will be somewhat dipolar but will have a significant higher order (quadrupole) moment. As a result, the field strength will vary highly non-linearly with distance and the signatures observed by MAG-A and MAG-B in step 3_1 will be asymmetric with respect to the time when the spacecraft is closest or furthest from the sensor. This results in a clear cusp-like peak in the field when the spacecraft is closest to the sensor and a smaller broad extremum when the spacecraft is furthest away (cf. Figure 17 below). Moreover, these signatures are exactly out of phase at MAG-A and MAG-B. The signatures in the MAG-FLR data were also asymmetric with respect to the direction of spacecraft displacement so once the direction of spacecraft displacement is established in step 3_1 from the MAG-A and MAG-B data, it is also known from the MAG-FLR data for step 3_2. The same analysis was applied to all steps to unambiguously determine the direction of spacecraft displacement throughout each step.

4. Results

Data from selected test steps are presented to illustrate the character of the data and the features used for comprehensive analysis and comparison with the model. The results are then quantitatively compared with calculations using the spacecraft model both including and excluding the cancellation magnets to demonstrate the sensitivity of the results to errors in the installation of the cancellation magnets.

4.1. Example Observations and Model Calculations

Figure 16 shows results from step 3_1. From top to bottom the panels show data from MAG-A, MAG-B and MAG-FLR. In each panel the color coding is red=X, green=Y and blue=Z and the axes are native magnetometer sensor coordinates. The MAG-B data were quite noisy and both the original and smoothed data are shown. The baselines for MAG-A and MAG-FLR were very stable during the test but were variable for MAG-B. The two series of free

pendulum swings are clearly identified and it is clear from the upper two panels that the spacecraft was displaced toward MAG-B and then released. The first free pendulum swing appears to be less reliable because the relative amplitudes of the difference components were not preserved through the seven oscillations whereas the second run preserved the relative amplitudes much better.

Figure 17 shows an expanded view of the second pendulum swing series from 3_1 but

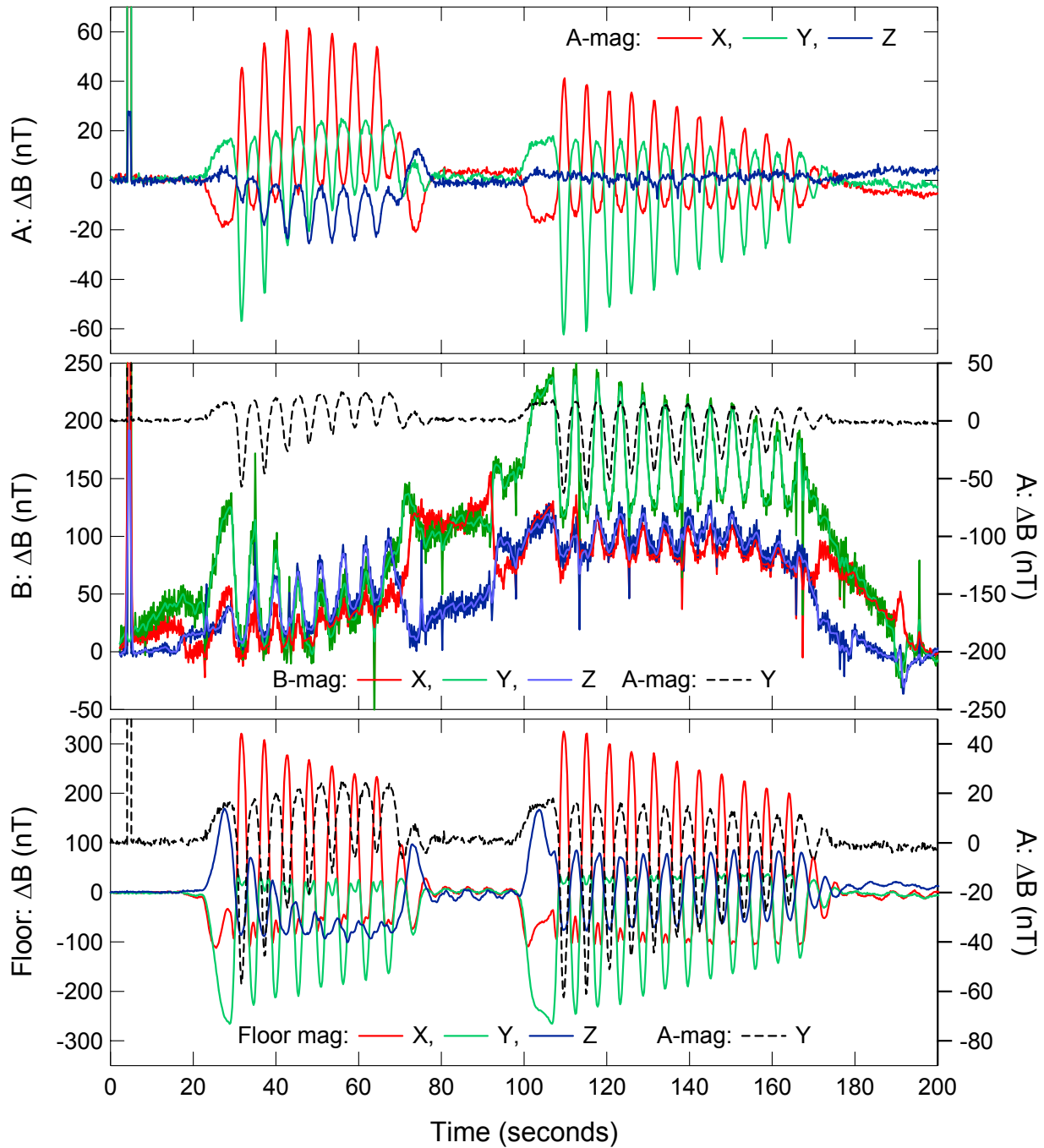


Figure 16. Test results from step 3_1 for all three magnetometers. The data for MAG-B have been time shifted to match the timing pulse in MAG-A. The Y-axis MAG-A data are reproduced in both the MAG-B and MAG-FLR data panels.

with the color coding changed to correspond to spacecraft coordinates for comparison with the model calculations. For MAG-B only the smoothed data are shown. It turns out that the Y magnetometer and Y spacecraft axes were parallel for both MAG-A and MAG-B so the green traces are the Y axes. The dashed curves in the middle and bottom panels are the MAG-A Y axis ($-Y_{SC}$). From the middle panel one can clearly see the cusp-like anti-phase signatures in the Y

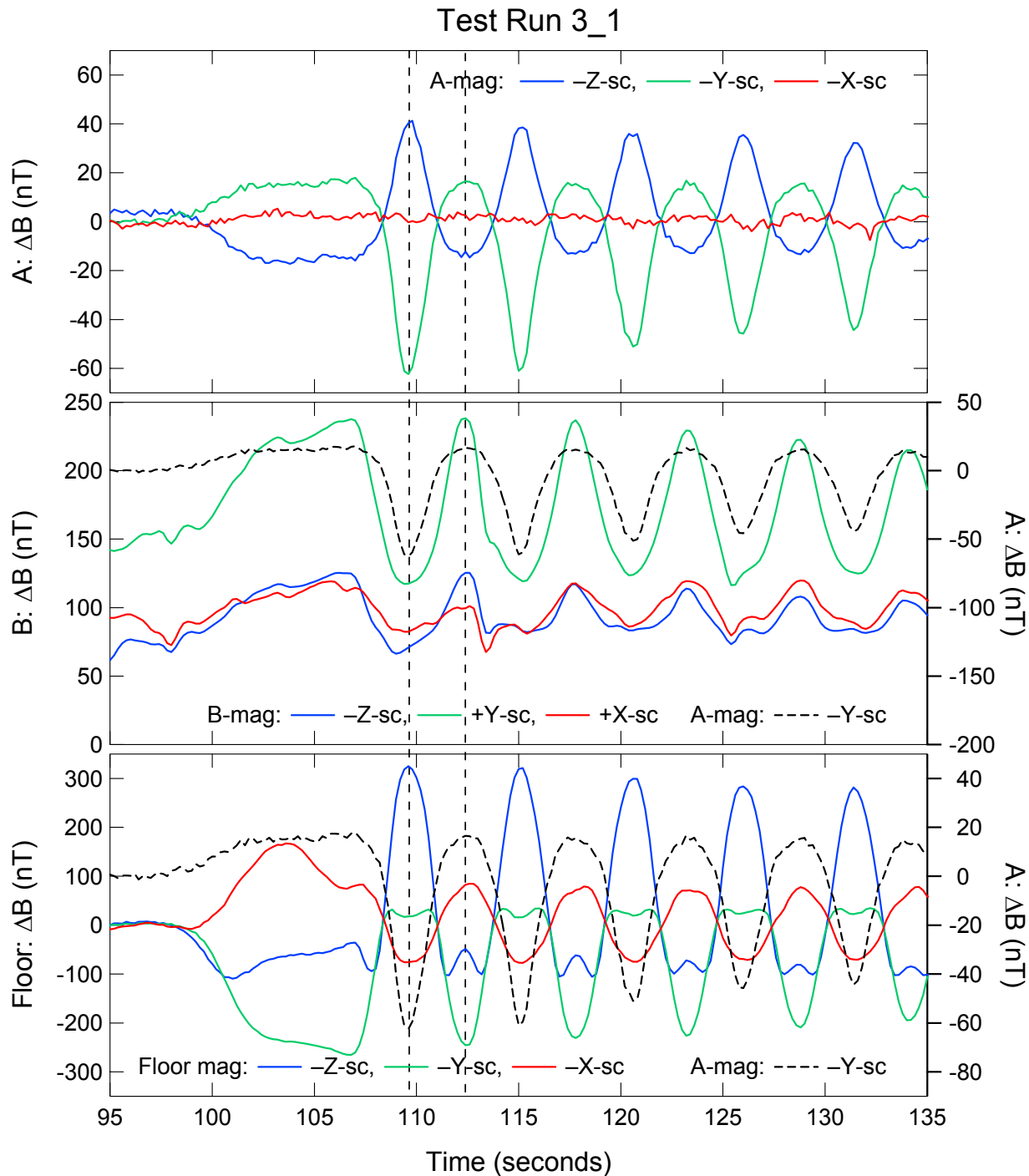


Figure 17. Expanded display of the second pendulum swing of step 3_1 in the same format as Figure 16 except that the color labels now follow spacecraft coordinates: red= X_{SC} , green= Y_{SC} and blue= Z_{SC} with sign differences indicated in the respective legend for each panel.

components of MAG-A and MAG-B. The dashed lines indicate times of closest approach to MAG-A (~109.5 s) and MAG-B (~112.5 s). The MAG-A and MAG-B time series have monotonic though asymmetric character indicative of a dipole or higher order field source moving toward and away from the sensor. By contrast, MAG-FLR observes non-monotonic signatures indicative of a structured field moving back and forth laterally. The local minima in the Z_{SC} and Y_{SC} components at opposite extrema in spacecraft displacement are significant signatures because they reflect the detailed structure of the field.

To evaluate the model field one needs to know the position of the magnetometer sensors in spacecraft coordinates at the extrema of the spacecraft displacements. At 109.5 s MAG-A and MAG-B are approximately at a Y_{SC} positions of $+236\text{ cm} - 60\text{ cm} = +176\text{ cm}$ and $-236\text{ cm} - 60\text{ cm} = -296\text{ cm}$, respectively (cf. Table 5). At 112.5 s MAG-A and MAG-B are roughly at $+296\text{ cm}$ and -176 cm , respectively. At 109.5 s and 112.5 s the Y_{SC} coordinate of MAG-FLR is -60 cm and $+60\text{ cm}$, respectively. Figure 18 shows the spacecraft magnetic field model evaluated along the approximate trajectories of the MAG-A sensor in spacecraft coordinates. The difference between near and far from the spacecraft is about $+60\text{ nT}$ in the Y-component and about -80 nT in the Z component. The X-component variation is fairly small. These results are in fair agreement with the top panel of Figure 17, the difference between maxima and minima in Y and Z are in the range 50 nT to 80 nT and the signs are as predicted by the model (note the negative signs in the labels of Figure 17). In addition, the X-component signal is quite small consistent with the model.

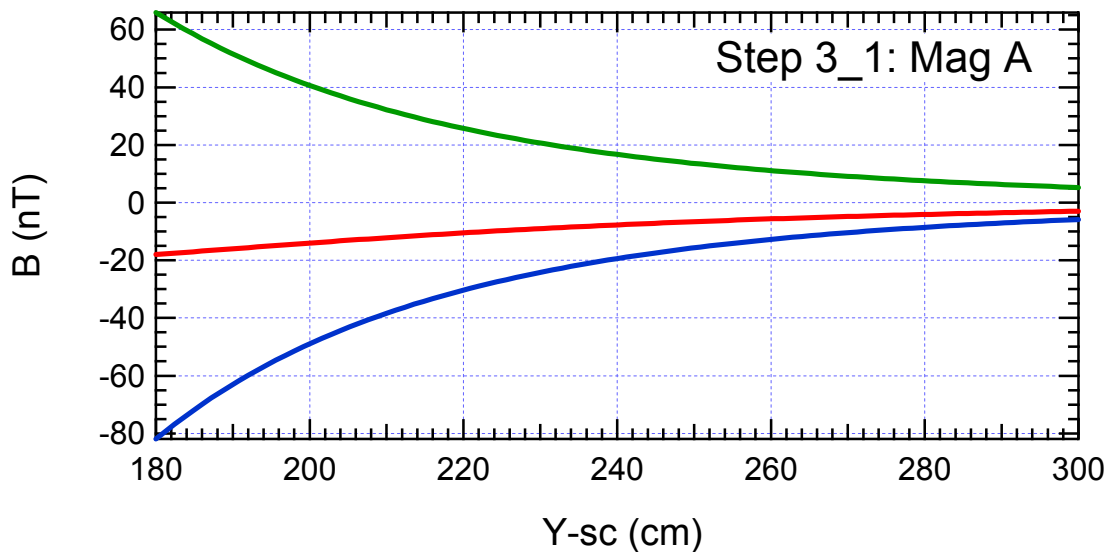


Figure 18. Spacecraft magnetic field model evaluated along the trajectory of MAG-A in spacecraft coordinates for step 3_1. Color coding is red = X_{SC} , green = Y_{SC} and blue = Z_{SC} .

Figure 19 shows the model evaluated for MAG-B in step 3_1 in the same format as Figure 18. In this case, both X and Y components should have larger positive values close to the spacecraft while Z should be very small. The middle panel of Figure 17 shows that both Y and Z are positive and the Y-component is about 100 nT larger close in, the X-component is only about 50 nT and the Z-component is comparable to X. Thus, although the signs are basically right, the relative magnitudes are not in as good agreement as for MAG-A.

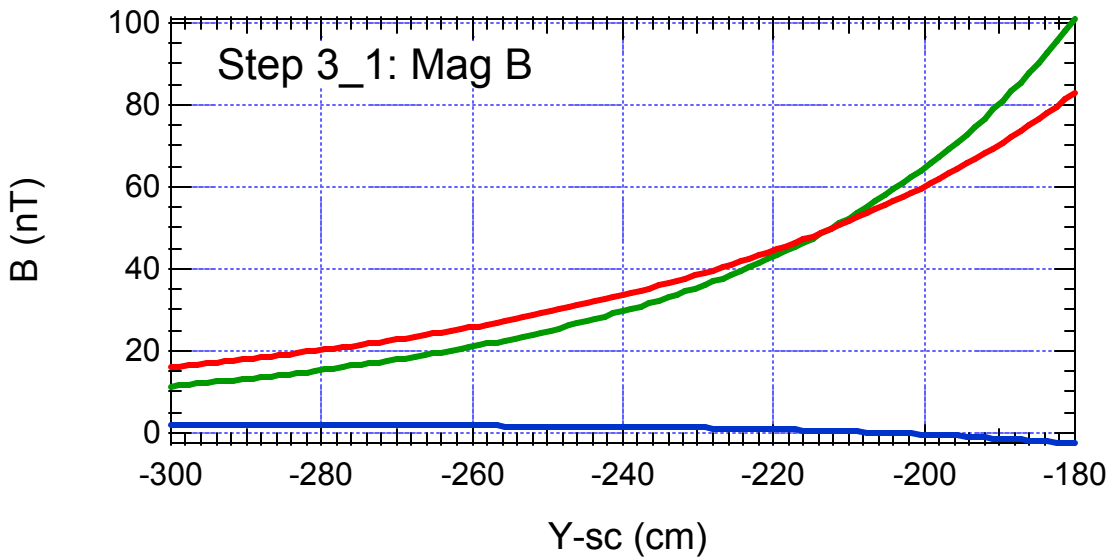


Figure 19. Spacecraft magnetic field model evaluated along the trajectory of MAG-B in spacecraft coordinates for step 3_1 in the same format as Figure 18.

Figure 20 shows the model evaluated now for MAG-FLR in step 3_1. Because the MAG-FLR baseline was very stable the departures from $Y = 0$ could be reliably measured in the observations so the model comparisons are made relative to the field at $Y = 0$. For negative Y (spacecraft toward MAG-A), the X, Y and Z components are positive, positive and negative, respectively relative to $Y = 0$ while the observations in the bottom panel of Figure 17 at 109.5 s give X, Y and Z positive, small negative, and large negative. At the other extreme, positive Y , the model predicts for X, Y and Z, negative, large positive and large positive which agree in all

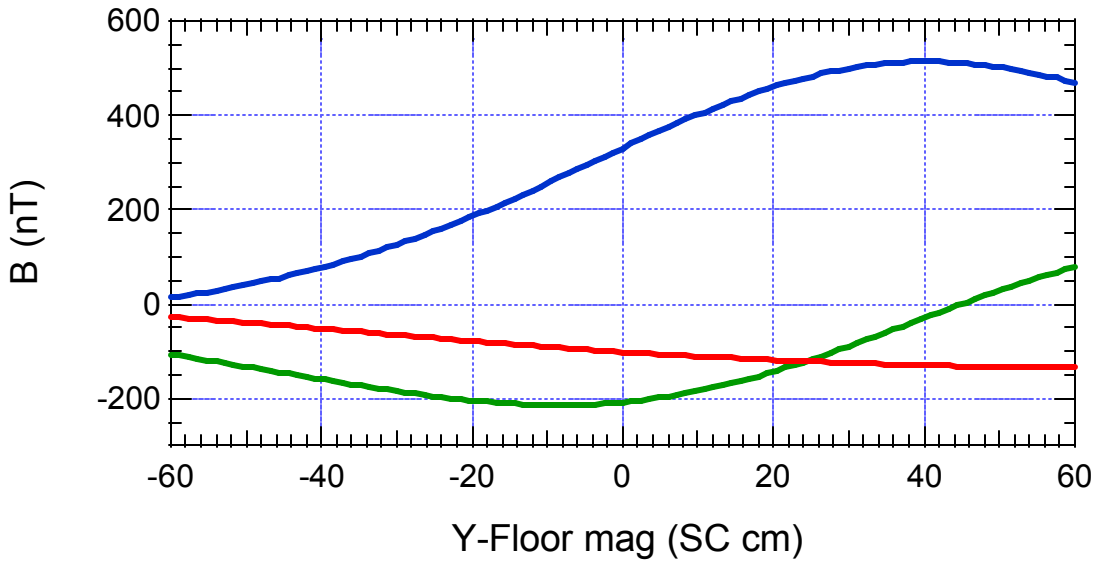


Figure 20. Spacecraft magnetic field model evaluated along the trajectory of MAG-FLR in spacecraft coordinates for step 3_1 in the same format as Figure 18.

components with the observations at 112.5 s. Moreover, the local extrema in Y and Z are reproduced in the model indicating that something very similar to the detailed structure in the model is actually observed.

4.2. Comprehensive Comparison

For each step the data were displayed in formats similar to those in Figure 17 and the differences between extrema of the first oscillation were recorded for MAG-A and MAG-B together with the displacements from baseline in the MAG-FLR data at the times of extreme positions of the spacecraft. The corresponding differences in each component were then evaluated from the field model. The accuracy of the measurements was estimated from the difference between the first and second set of pendulum oscillations for each step. It was found that the differences in spacecraft coordinates for the 0° and 180° orientation were identical to

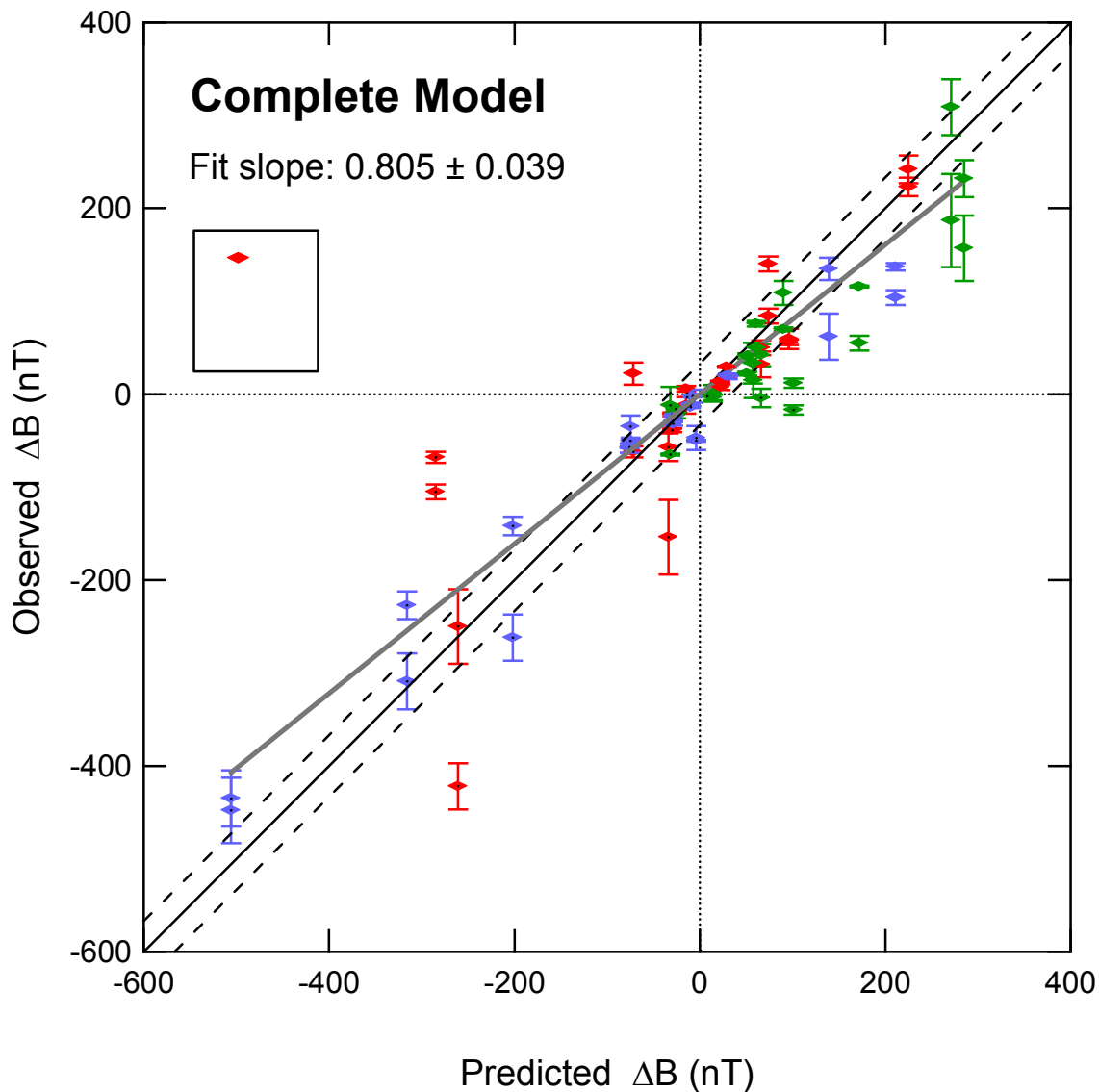


Figure 21. Observed magnetic field differences versus corresponding differences predicted using the spacecraft magnetic field model. Components in spacecraft coordinates are color coded as indicated.

within the accuracy of the determinations indicating that the magnetic field is predominantly due to permanent magnets of the spacecraft rather than to moments resulting from permeable materials in Earth's field. Moments due to permeable materials are fixed relative to the Earth's magnetic field and do not rotate with the spacecraft whereas permanent magnets rotate with the spacecraft.

To compare the model and observations for all tests the observed field differences are plotted versus the model predictions in Figure 21. The error bars indicate the variance between determinations for the same step. The thin solid line shows a slope of unity passing through the origin and the thin dashed lines indicate departures above and below the line corresponding to three times the average 1-sigma estimates of the measurement uncertainties. The thick gray line shows the linear fit constrained to pass through the origin having the slope indicated. The regression coefficient was +0.93. Figure 22 shows the observations plotted versus the results

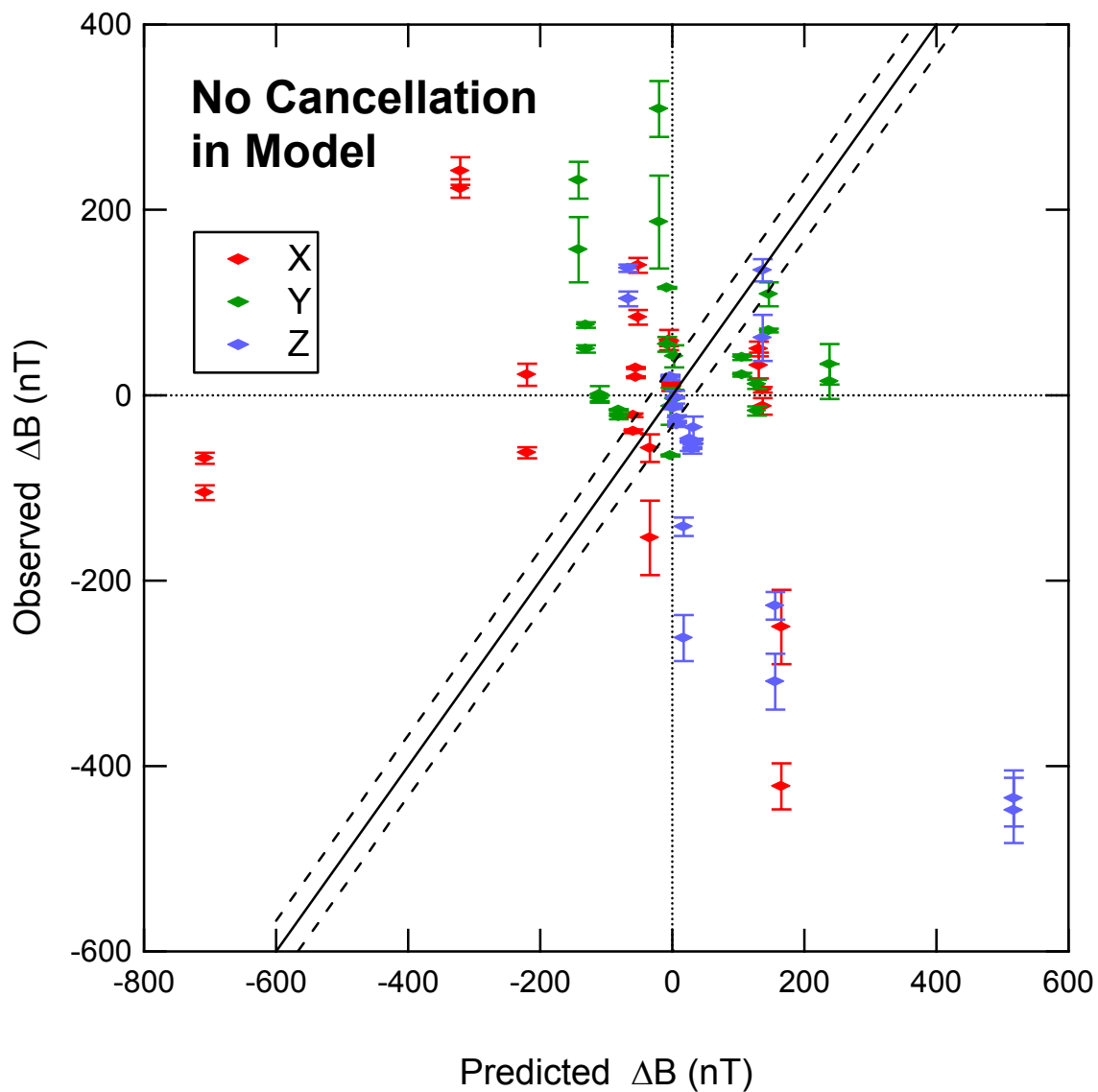


Figure 22. Observed magnetic field differences versus corresponding differences predicted using the spacecraft magnetic field model excluding the cancellation magnets. The format is the same as Figure 21 except no regression line between the observations and model is given.

from the model excluding the cancellation magnets. The disparity between the model without the cancellation magnets is dramatic. In fact, the regression coefficient is -0.38 indicating strong disagreement between the observations and the model without the cancellation magnets. The results therefore provide strong confirmation that the cancellation magnets were installed properly.

In addition to the comparison in Figures 21 and 22, it is informative to compare the angle between the model and observed field changes as well as the magnitude of the field change. These are shown in Figure 23, solid symbols for the complete model and open symbols

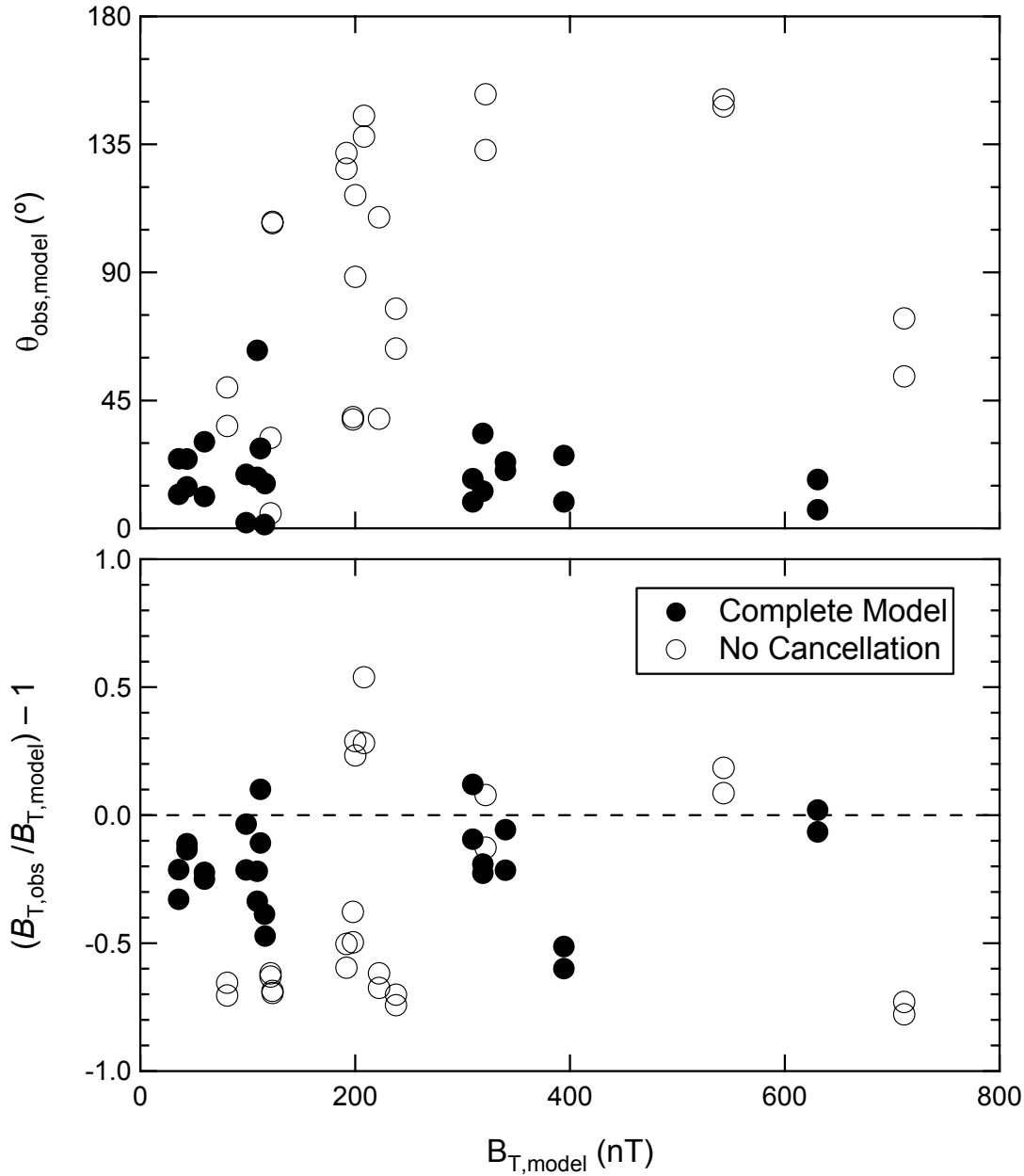


Figure 23. Comparison of observed and model field changes showing the angle between the models and observations (top) and the relative difference in the magnitude of the field difference (bottom).

for the model without the cancellation magnets. The complete model agrees in direction with the observations generally to within 30° whereas the model without cancellation magnets points in the opposite direction ($>90^\circ$ difference) in half of the cases. The observed magnitude of the field difference is on average 20% lower than the complete model. The model without the cancellation magnets is generally in strong disagreement with the observations.

Both the components, Figure 21, and the magnitude of the field difference indicate that the observations are about 20% low relative to the complete model while the directional agreement is quite good. The model calculations all assumed a 24" displacement of the spacecraft without any rotation. In actuality only the laser spot on the floor was displaced 24" while the spacecraft displacement at the height of MAG-A and MAG-B is less. Estimating the height to the crane above the floor to be 30', and using the heights of MAG-A and MAG-B from Table 5, 90 cm, the displacement at the heights of MAG-A and MAG-B is closer to $60 - 2/30 \cdot 90 = 54$ cm, or 10% less. Since a dipole field varies as $1/d^3$, this could account for as much as a 30% smaller signal than the model calculations. One can also estimate the effect of a 6 cm smaller displacement from Figures 19 and 20. The 20% systematic difference is therefore considered to be within the probable bias in the test and model comparison and we conclude that the observations are in agreement with the model to at least 20%.

5. Conclusions

The test results are best considered in terms of the test objectives: (1) to establish that all major sources of fixed magnetic fields had been identified; (2) to verify that the cancellation magnets were installed properly; (3) to test the spacecraft magnetic field model. The excellent quantitative agreement with the model and the dramatic disagreement that results if the cancellation magnets are removed from the model confirms all three objectives. Since the magnetometer boom will remain stowed for the first phase of cruise, through the Earth fly-by, it is important to estimate the magnetic field we expect to observe in the stowed position. The magnetometer sensor center of mass in the stowed position in spacecraft (X, Y, Z) coordinates is (0, 104, -198) cm. In the spacecraft field model this gives a field, $\mathbf{B}_{SC-Stowed} = (+155, +3, +154)$ nT in spacecraft coordinates. The conversion between sensor and spacecraft coordinates when stowed is $X_{MAG}=X_{SC}$, $Y_{MAG}=-Z_{SC}$, $Z_{MAG}=Y_{SC}$ so the field in sensor coordinates should be $\mathbf{B}_{MAG-Stowed} = (+155, -154, +3)$ nT. We therefore expect to be able to operate the magnetometer in its sensitive range (± 1024 nT full scale) in the stowed configuration which will allow optimal assessment of the spacecraft noise during the first segment of the cruise phase. This will also simplify monitoring boom deployment since we will be able to use the sensitive range throughout the deployment process.

6. Relevant Documents

MESSENGER Propulsion Latching Valve Magnetic Moment Measurements, B. J. Anderson and H. Korth, 4 June 2002.

JHU/APL Document 7384-9925 MESSENGER S/C Magnetic Characterization Procedure.

JHU/APL Document 7384-9135 Handling Plan at APL MESSENGER.